FLORE
Repository istituzionale dell'Università degli Studi di Firenze

STRUCTURAL MAGNETIC CORRELATIONS IN PHASE-TRANSITIONS OF MOLECULAR MAGNETS

(Article begins on next page)

STRUCTURAL MAGNETIC CORRELATIONS IN PHASE TRANSITIONS OF MOLECULAR MAGNETS

ANDREA CANESCHI, DANTE GATTESCHI, ROBERTA SESSOLI

Department of Chemistry
University of Florence
Florence, Italy

ABSTRACT. The general conditions which must be met in order to achieve magnetically ordered phases are briefly reviewed. The magnetic ordering observed in linear chain compounds based on metal hexafluoroacetylacetonates and nitronyl nitroxides is related to their structural features. Mention is also made to the experimental techniques which allow the understanding of the preferred spin alignment. Possible developments of useful associations of properties in magnetic molecular materials are discussed.

1. Introduction

Several different approaches are currently used in order to design and synthesize molecular based materials exhibiting spontaneous magnetization (molecular ferromagnets) [1–8]. In principle these materials can be imagined to be formed assembling individual paramagnetic moieties which must be properly ordered in a three–dimensional lattice. According to the nature of the molecules the approaches can be classified as organic, organic–organometallic, organic–inorganic, and inorganic. Examples of all these types of approaches will be found in the Chapters of this book. Here we want to show how much is understood of the conditions which are needed in order to obtain molecular based materials exhibiting spontaneous magnetization, and which structural magnetic correlations must be established in order to achieve this goal.

The first structural correlation is intrinsic to the nature of magnetism, which requires a three–dimensional network of magnetic centers connected by appropriate exchange interactions [9]. Ideally one should assemble the molecules in a lattice with a number of nearest neighbors to which they are coupled ferromagnetically. Unfortunately it is relatively easy to assemble the molecules in chains, within which strong nearest neighbor exchange interactions can be active, but up to now no really three–dimensional magnetic lattices have been obtained. Since one–dimensional, and two–dimensional, magnetic materials do not sustain long range order [10], the possibility to observe magnetic phase transitions in compounds with a chain structure is determined by inter–chain interactions, which allow a cross–over to a three–dimensional magnetic structure. Therefore it is necessary to establish correlations between the magnetic properties of chains with those of the bulk lattices, in order to understand which mechanisms are responsible of the magnetic order at low temperature.

In the following we will focus essentially on the structural magnetic correlations in systems which we have designed and synthesized using metal ions and organic radicals as building blocks. We will resume first some typical properties associated with magnetically ordered materials which are needed in order to understand in some detail the mechanism according to which a molecular based solid can undergo a transition to magnetic order. Second we will show under which conditions strong intrachain interactions are observed, and which experimental techniques are useful in order to investigate the properties of one-dimensional materials in the paramagnetic state. Third we will show our understanding of the nature of the interchain interactions which can eventually lead to magnetic order. Finally we will show how how molecular based materials can show magnetic properties which are much different from those commonly met in traditional magnets, and how these properties can be understood on the basis of the structural features of the compound.

2. Magnetic Ordering and Magneto-Crystalline Anisotropy

One of the fundamental aspects of bulk magnetism is magneto-crystalline anisotropy, which determines the actual preferred spin orientation in the lattice and largely affects the properties of the magnetically ordered material [11].

In fact when one draws arrows to represent spins implicitly refers to magneto-crystalline anisotropy. In most molecular materials exchange is essentially Heisenberg type, which means that it only fixes the relative orientation of the spins, namely parallel or antiparallel to each other. In order to introduce directional properties it is necessary to take into account single center anisotropy effects and anisotropic and antisymmetric spin-spin interactions [12]. These are given by both through-bond and through-space interactions. The former is determined by exchange involving the ground states and the excited states mixed in by spin-orbit coupling. The through-space component is determined by magnetic dipolar interactions. The appropriate theory can be found elsewhere [12,13].

In general limiting to bilinear interactions, the spin hamiltonian appropriate to the interactions between two spins S_1 and S_2 can be written as:

$$H = J \, S_1 \cdot S_2 + S_1 \cdot D_{12} \cdot S_2 + d \cdot S_1 \times S_2 \qquad (1)$$

The first term is isotropic and generally is largely determined by Heisenberg exchange. The second term, where D_{12} is a traceless matrix, is anisotropic. In the simple case of axial anisotropy this term can give preferential orientation of the spins along the line connecting them when $|D_{zz}| > |D_{xx}|$, or orthogonal to this line when $|D_{zz}| < |D_{xx}|$. In the former case for $D_{zz} < 0$, and antiparallel to each other for $D_{zz} > 0$. Analogous considerations can be made for the latter case, provided D_{xx} is substituted to D_{zz}.

The third term in (1) is antisymmetric and it tends to orient the spins at 90° from each other.

The other relevant anisotropic terms which must be taken into account are of the type:

$$H = S_1 \cdot D_1 \cdot S_1 + S_2 \cdot D_2 \cdot S_2 \qquad (2)$$

and they are determined by the anisotropy of the crystalline field around the two spin centers 1 and 2.

The magneto-crystalline anisotropy is the result of the application of (1) and (2) to the whole lattice. It provides the relative orientation of the arrows on neighboring centers, and also their absolute orientation in the lattice in the absence of an external magnetic field. The knowledge of magneto-crystalline anisotropy would be very important to a detailed understanding of the magnetic properties of magnets, but it must be obtained from experiment, because it is still practically impossible to calculate it from first principles.

The existence of non-isotropic terms in (1) and (2) determines the fact that the angle between neighboring spins is different from 0° and 180°. This is particularly relevant to antiferromagnets, in which small deviations from 180° make the compensation of the magnetic moments in the two different sublattices not perfect, thus providing a non-zero magnetization. Materials which behave like this are weak ferromagnets.

The preferred spin orientation may correspond to one direction, and in this case it is generally referred to as Ising anisotropy, or to a plane, and this is XY anisotropy. Systems with Ising anisotropy are magnetically one-dimensional, those with XY anisotropy are two-dimensional, and Heisenberg systems are three-dimensional.

Magnetic dimensionality affects the critical temperature, i.e. the temperature below which magnetic order is established. All parameters remaining the same an Ising magnet orders at higher temperature than a XY magnet [10]. In Figure 1 the spin correlation length ξ is plotted for Ising, XY, and Heisenberg one-dimensional magnets. It is apparent that, with the same value of the coupling constant J, at a given temperature T, ξ is much higher for Ising than for Heisenberg magnets.
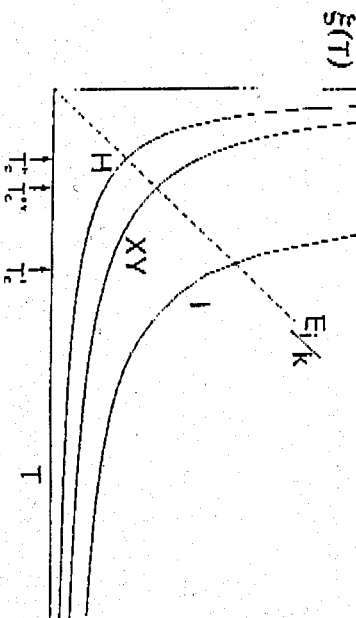

Figure 1. Correlation length ξ for Ising, XY and Heisenberg magnets. The intersection of the dotted line with the curves yields the critical temperature.

A simple model suggests that the critical temperature is related [14] to the spin correlation length by:

$$kT_c = E_1 \, \xi(T_c) \quad (3)$$

where E_1 is an energy associated with the interactions between the chains. Equation (3) admits the graphic solution shown in Figure 1. Ising magnets have higher transition temperatures than Heisenberg magnets.

3. One-Dimensional Metal-Nitroxyl Nitroxide Magnets

3.1 Structural Types

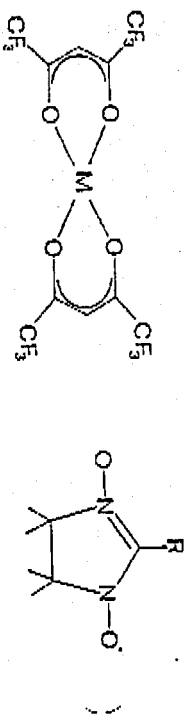Linear chain compounds can be synthesized using $M(hfac)_2$ and NITR building blocks [15], shown in Figure 2.

Figure 2. The $M(hfac)_2$ and NITR building blocks for molecular magnets.

We have found that the NITR radicals can bridge two metal ions with two NO groups both in a $\mu-1,3$ fashion or in a $\mu-1,1$ fashion, as shown in Figure 3.
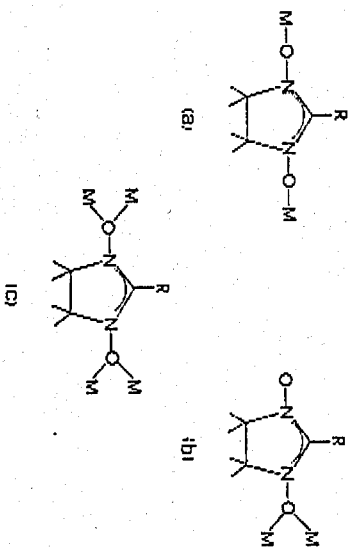
Figure 3. Possible coordination modes of the NITR radicals.

For the $\mu-1,3$ coordination, linear chains can be formed according to the schemes of Figure 4a and 4b, respectively. For a *trans* coordination of the two

radicals around the metal ion straight chains can be formed, while for *cis* coordination staircase structures are obtained. Eventually spiral staircases can be formed.
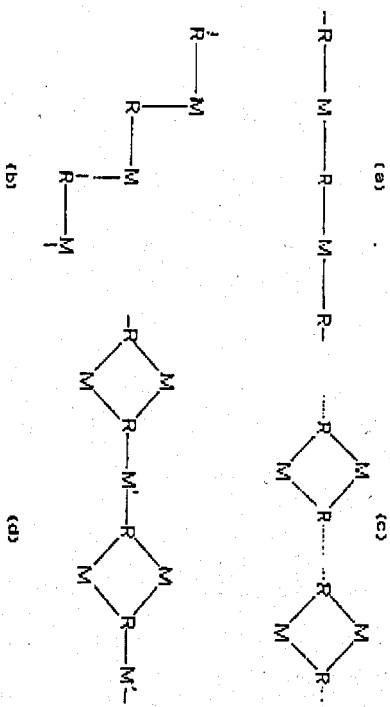
Figure 4. Types of extended structures observed for compounds formed by $M(hfac)$ and NITR building blocks.

For $\mu-1,1$ coordination linear chain compounds can be formed as shown in Figure 4c. In this case the NO group which is not bound to the metal ion interacts with the analogous NO group of another molecule.

The coordination scheme of Figure 3c has been only postulated [16], and in this case a two-dimensional magnetic structure can be formed.

The linear chain compounds of Figure 4d are formed when an additional donor atom is present on NITR. For instance when R= py, the radical acts as a tridentate ligand and $[Cu(hfac)_2]_3(NITpPy)_2$ has in fact that structure [17].

Chains of type a and b can be ferromagnetic or ferrimagnetic, depending on the sign of the exchange interaction, if the metal ion M is magnetic. If the metal ion is non-magnetic both ferro- or antiferro-magnetic chains can be formed. We have experimentally found examples of all these types of behavior [15].

In the chains of the type depicted in Figure 4c in general the radical-radical exchange interaction is antiferromagnetic, so one-dimensional antiferromagnets result. If the M-R coupling is antiferromagnetic the M_2R_2 clusters form ferrimagnetic rings, while if the M-R coupling is ferromagnetic, ferromagnetic rings are formed. Experimentally we have found examples of the former but not of the latter type [15].

Chains as depicted in Figure 4d can give raise to many different types of behavior depending on the sign of the metal-radical coupling constants.

3.2 Paramagnetic Properties

We have investigated the one-dimensional antiferromagnets

Zn(hfac)$_2$(NITPr)(H$_2$O) [18], Y(hfac)$_3$(NITEt) [19] Rey et al reported the magnetic properties of Rh$_2$(tfac)$_4$(NITPh) [20]. The last two have a structure which can be correlated to the scheme of Figure 4a, while the first has the structure shown in Figure 5. The exchange pathway goes through yttrium(III) in Y(hfac)$_3$(NITEt), through the Rh$_2$(tfac)$_4$ dimers in Rh$_2$(tfac)$_4$(NITPh), while it goes presumably through a direct interaction between the NO groups which are connected by a dotted line in Figure 5 for Zn(hfac)$_2$(NITPr)(H$_2$O). The isotropic coupling constant is 4.5 cm^{-1} for the first, 97 cm^{-1} for the second, and 12.2 cm^{-1} for the third. The data were fitted with the usual formula for one-dimensional Heisenberg antiferromagnets [20].
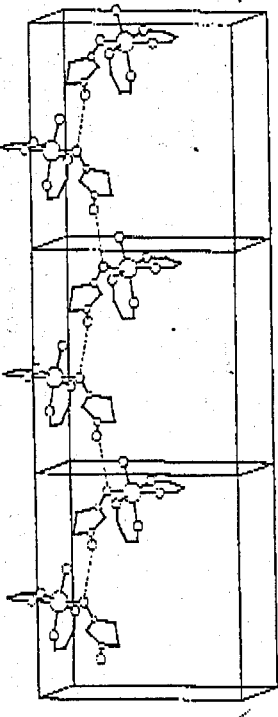
Figure 5. Structure of the chains in Zn(hfac)$_2$(NITPr)(H$_2$O)

It is extremely interesting to remark here that if NITPh in Rh$_2$(tfac)$_4$(NITPh) is substituted by the analogous IMMe radical whose formula is shown in Figure 6, the resulting chains are ferro– [21] rather than antiferromagnetic.
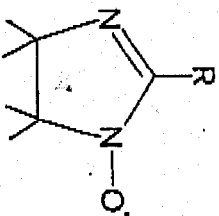
Figure 6. Formula of the IMMe radical.

The reason for the different behavior is that while the magnetic orbitals of the nitronyl nitroxides are efficiently coupled by the σ orbitals of Rh$_2$(tfac)$_4$, the π* orbitals of the imino-nitroxides are orthogonal to the σ orbitals of Rh$_2$(tfac)$_4$ thus

yielding a ferromagnetic coupling corresponding to J= −4 cm^{-1} [21]. Rh$_2$(tfac)$_4$(IMMe) is an example of a one-dimensional organic ferromagnet, because the metal ions only provide a rigid frame to the chains, and an efficient superexchange pathway to the radical π* magnetic orbitals.

The EPR spectra of Zn(hfac)$_2$(NITPr)(H$_2$O) [18] and Y(hfac)$_3$(NITEt) [19] have typical one-dimensional behavior which shows up in deviations of the lineshape from lorentzian behavior, in the angular dependence of the linewidth which follows a $(3\cos^2\phi-1)^n$ dependence around the chain direction, and in g shifts at low temperature, which are determined by short range order effects [22,23].

The typical one-dimensional behavior can be destroyed by several perturbations. Among these inter-chain exchange interactions play a major role, as is intuitively clear, because a large inter-chain coupling will change the system from one– to two– or three-dimensional. The lineshape is the spectral parameter which is more readily affected by inter-chain exchange interactions, which begin to show their effects when J'/J < 10^{-3}. The determination of the lineshape of the EPR spectra of a one-dimensional magnetic material can therefore be an important information for the structural characterization of the material.

The g shifts observed at low temperature are also particularly important in order to recognize which are the preferred spin directions. In fact when the exchange energy becomes comparable with thermal energy the spins along the chain become correlated in relatively long segments, and internal fields thus generated either add or subtract to the external field of the EPR spectrometer [24]. As a consequence the resonance shifts down– or up-field, according to the spin orientation. For both ideal ferro– and antiferro–magnets the resonance shifts down-field parallel to the chain, and up-field orthogonal to it. For ideal ferrimagnets the pattern is completely reversed. Ideal one-dimensional magnet here means a linear chain system in which the possible interaction are nearest neighbor exchange and dipolar interactions. Ideal ferromagnets have Ising anisotropy, while both ferri– and antiferro–magnets have XY anisotropy [23]. The g shifts are related to the magnetic anisotropy according to the relation [25]:

$$B_j = \sqrt{\chi_j \chi_k / \chi_i}\, B_0 \quad (4)$$

where i, j, k correspond to x, y, and z, B$_0$ is the resonance field in the absence of short range order effects, and B$_i$ is the resonance field along i. The values appropriate to the other directions can be obtained by cyclic permutations.

Equation (4) states that the type of information which can be obtained from magnetic anisotropy and single crystal EPR spectra is essentially the same. However, in general for the latter experiment smaller crystals are required, which can be extremely important for molecular based materials, which are often reluctant to yield big crystals. Finally it must be recalled that even polycrystalline powder EPR spectra can yield useful information on the nature of the magneto-crystalline anisotropy.

The extent of the g shift depends on the dipolar and exchange energies [24], in the sense that an increase of both induces larger shifts. Chains with larger spins tend to give larger g shifts than chains with smaller spins.

Detecting the g shifts in one dimensional S= 1/2 antiferromagnets is not simple. We succeeded in doing that for Zn(hfac)$_2$(NITPr)(H$_2$O) only by using a high field spectrometer operating at 248 GHz [18]. The temperature dependence of the g shifts of Zn(hfac)$_2$(NITPr)(H$_2$O) is shown in Figure 7. The experimental

data clearly show that the anisotropy is of the XY type, as expected for an ideal one-dimensional antiferromagnet. The reason why the shifts are so small is that the dipolar interaction is rather weak because the spins on the chain are fairly distant from each other and the intra-chain coupling is also small.
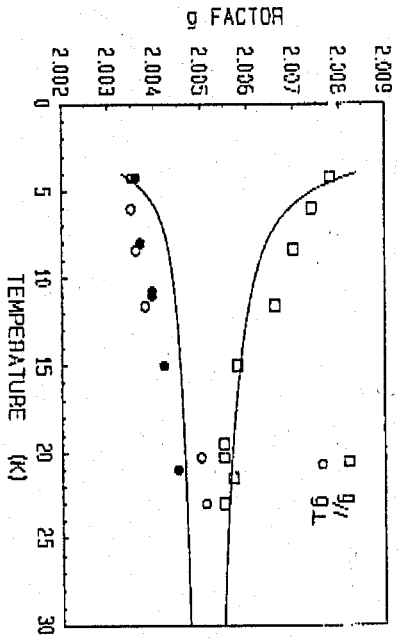

Figure 7. Temperature dependence of the g shifts for $Zn(hfac)_2(NITiPr)(H_2O)$. The filled circles refer to single crystal spectra.

Cu(hfac)$_2$(NITR) chains behave as one-dimensional ferromagnets as shown by EPR and magnetic measurements [26,27]. The origin of the ferromagnetic coupling between copper(II) and the radical is the fact that the magnetic orbitals of the two magnetic centers are orthogonal to each other when the radical occupies an axial position in the distorted octahedral coordination around copper(II). The exchange coupling constants were found to be in the range $J= -20$ to -25 cm^{-1}. The EPR spectra of both Cu(hfac)$_2$(NITMe) and Cu(hfac)$_2$(NITiPr) have one-dimensional behavior of the linewidth [27,28], but the lineshape is lorentzian, due to the slightly zig zag nature of the chain, and to the presence of anisotropic exchange contributions. The low temperature EPR spectra show sizeable g shifts which show that the preferred spin orientation is parallel to the chain in agreement with the ferromagnetic nature of the materials.

Ferrimagnetic chains are formed by manganese(II) [29-31] and nickel(II) [32] because the coupling constant between metal and radical is in this case antiferromagnetic. The sign of the coupling constant is readily understood if one considers that for nickel(II) and manganese(II) there is at least one magnetic orbital on the metal ion which can overlap to the radical magnetic orbital.

The temperature dependence of the magnetic susceptibility for one-dimensional ferrimagnets can be calculated with several models of various sophistication. The simplest approach is the Ising approach [33] which however is not realistic for this kind of spins. In the opposite limit all the spins are treated as classical spins [34], and formulae are also available which treat the S= 1/2 spins as quantum spins, and the others as classical spins [35]. Finally for chains with

$S_1=1/2$ and $S_2= 1$ the susceptibility has been calculated through a procedure of extrapolation using small rings [36].

The values of the coupling constants are in the range $J \simeq 400$ cm^{-1} for the nickel [32] and $J \simeq 200- 350$ cm^{-1} for the manganese derivatives [29-31]. These values, coupled with the relatively large value of the nickel(II) and manganese(II) spins, yield high correlation lengths of the spins at low temperatures, which show up in the high values of χT. In Figure 8 the temperature dependence of χT is shown for Mn(hfac)$_2$(NITiPr). The correlation length can be approximately calculated as:

$$\xi(T)= \chi(T)/\chi_c(T) \, (S+1)/S - 1/S \qquad (5)$$

where $\chi(T)$ is the susceptibility of the one-dimensional material, $\chi_c(T)$ is the susceptibility of an analogous compound following the Curie law, and S= 2 for the manganese, S= 1/2 for the nickel derivative. In this way correlation lengths of 50-60 metal ions are calculated at low temperature.
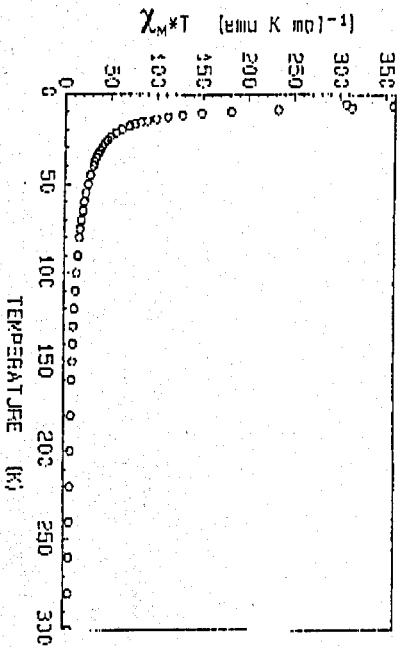

Figure 8. Temperature dependence of χT for Mn(hfac)$_2$(NITiPr).

The manganese compounds are the ones more intensively investigated. Mn(hfac)$_2$(NITiPr) has a straight chain structure [29] corresponding to Figure 4a, while Mn(hfac)$_2$(NITiPr), Mn(hfac)$_2$(NITEt) [31], and Mn(hfac)$_2$(NITPhOMe) [37] have the stepped structure of Figure 4b. In particular Mn(hfac)$_2$(NITPhOMe) has a spiral staircase structure imposed by a crystallographic 3_1 symmetry of the chains.

The structural differences in the four compounds are clearly reflected in the EPR spectra. Mn(hfac)$_2$(NITiPr), which has a regular chain structure, has typical one-dimensional behavior at room temperature [29], while the other three compounds, which have a stepped chain structure, do not show any of the one-dimensional features at room temperature [31,37]. However all of them show sizeable g shifts at low temperature, which provide useful information on the preferred spin orientation.

Mn(hfac)$_2$(NITiPr) has a quasi XY type of anisotropy, with the spins which orient in the plane perpendicular to the chain in agreement with an almost ideal one-dimensional structure. A perfect XY type of anisotropy is shown by Mn(hfac)$_2$(NITPhOMe), while Mn(hfac)$_2$(NITiPr) and Mn(hfac)$_2$(NITEt) have a quasi Ising type of anisotropy. The difference between these compounds is bound to the fact that crystallographic symmetry imposes that in Mn(hfac)$_2$(NITPhOMe) the plane orthogonal to the trigonal axis is isotropic, and since the interplay of antiferromagnetic exchange and dipolar interactions pulls the spins out of the chains, the result is XY anisotropy. In Mn(hfac)$_2$(NITEt), and Mn(hfac)$_2$(NITiPr) the stepped chains lie approximately in a plane, and the spins orient preferentially orthogonal to this plane where the most intense dipolar interactions are observed. Therefore the resulting anisotropy is of the Ising type. Extremely large g shifts were observed for Mn(hfac)$_2$(NITEt): at 10 K the g value reaches 3.8.

4. Three-Dimensional Metal–Nitronyl Nitroxide Magnets

4.1 Manganese Chains.

Mn(hfac)$_2$(NITnPr), Mn(hfac)$_2$(NITEt), Mn(hfac)$_2$(NITiPr), Mn(hfac)$_2$(NITPhOMe), represent the most complete series of metal–radical one-dimensional compounds whose transition temperatures have been accurately investigated [30,31,37], and which allowed us to establish some useful structural–magnetic correlations.
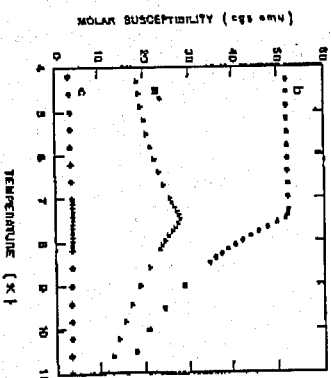
MOLAR SUSCEPTIBILITY (emu cgs)

TEMPERATURE (K)

Figure 9. Temperature dependence of the magnetic susceptibility of Mn(hfac)$_2$(NITiPr) in an external field of 0.5 G.

All these compounds undergo a transition to three-dimensional ferromagnets in the range 5–9 K, in which three-dimensional order corresponds to a ferromagnetic ordering of ferrimagnetic chains. In Figure 9 the magnetic susceptibility of Mn(hfac)$_2$(NITiPr) in an external field of 0.5 G is shown. A singularity is observed at $T \cong 7.5$ K, indicative of a magnetic phase transition. The susceptibility was found to follow the critical law:

$$\chi = \Gamma (T - T_c)^\gamma \qquad (6)$$

with $T_c = 7.61$ K and $\gamma = 1.13$. The critical exponent depends on the type of magnet which is considered. For a Heisenberg 3-D ferromagnet $\gamma = 1.38$, while for a uniaxial dipolar ferromagnet $\gamma = 1$ [10]. Our observed value puts Mn(hfac)$_2$(NITiPr) closer to the latter limit, and also other evidences, to be discussed below, suggest that indeed it is the dipolar interaction between the chains which drives the 3-D magnetic ordering.

The saturation magnetization of Mn(hfac)$_2$(NITiPr) corresponds to ca. 4 BM, in good agreement with the value expected for a $S=2$ spin. This value is determined by the fact that the manganese–radical pairs are strongly antiferromagnetically coupled to give a ground $S= 2$ state.

Similar results were observed for the other manganese–radical chains, whose critical temperatures are collected in Table I. In particular Mn(hfac)$_2$(NITEt) yielded the hysteresis loop shown in Figure 10. Apparently these manganese radical compounds behave as soft magnetic materials.
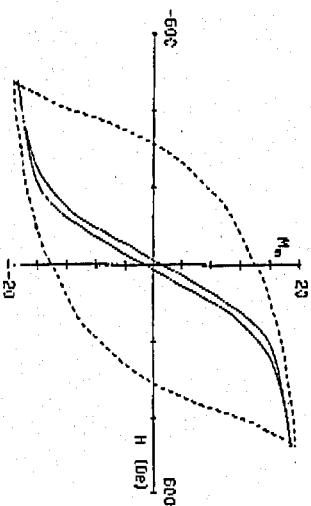
M_n

H (Oe)

Figure 10. Hysteresis loop for Mn(hfac)$_2$(NITEt) at 4.2 K (—) and 1.25 K (---). The molar magnetization is given in (emu mol^{-1} G)/10^3.

In order to understand the origin of the differences in the critical temperatures for these compounds it is useful to take equation (3) as a reference point. The origin of the interaction energies E_j must preliminarily be established. The magnetic anisotropy of these compounds in the ordered phase follows the pattern observed in the paramagnetic phase. Since the preferred spin orientation is well understood on the basis of dipolar interactions, it seems reasonable to assume that indeed the driving force to 3-D order is the dipolar interaction.

A support to this hypothesis comes from the lack of any reasonable inter-chain exchange interactions in these compounds. In order to check if direct exchange interactions are possible, we must first look at which are the atoms of the Mn(hfac)$_2$ and NITR building blocks which have the largest unpaired spin density. These are of course the manganese ions and the NO groups of the nitronyl nitroxides, but in no compounds are inter-chain distances shorter than 8 Å observed. Shorter contacts are observed between CF$_3$ groups but these are considered to be magnetic insulators, therefore rather ineffective in transmitting superexchange interactions.

Table 1. Intra-chain Coupling, Dipolar Energies, and Calculated and Observed Critical Temperatures for Mn(hfac)₂(NITR) Chains.

Radical	J	E_d^x	E_d^y	E_d^z	T_c^c	T_c^o
NITPhOMe	344	-.063	-.063	.126	6.1	4.8
NITiPr	330	-.149	-.126	.265	8.8	7.6
NITEt	258	-.155	.063	.092	8.1	8.4

J is in cm⁻¹, dipolar energies and critical temperatures in K. Critical temperatures have been calculated with eq. 3. z corresponds to the chain axis. y corresponds to the b axis for NITiPr, while it is in the Mn-radical plane in NITEt.

The EPR spectra of the Mn(hfac)₂(NITR) family show that $J'/J << 10^{-3}$, thus concurring in the identification of the dipolar interaction as the responsible of the magnetic ordering. NMR spectra recorded at room temperature show spin diffusive behavior which is cut off at a frequency of ca. 20 MHz [38]. This value corresponds well to that expected for intra-chain dipolar interaction, and sets the J'/J limit even lower than 10^{-5}.

The dipolar energy can be calculated to a good approximation in a rather simple way. Focusing on a manganese-radical pair one can include the interaction with all the spins which are contained in a sphere centered around the reference pair. A radius large enough to ensure that the slowly decaying dipolar interactions are effectively quenched is 70 Å. The spins are oriented parallel to some particular direction, for instance parallel and perpendicular to the chain, and kept parallel or antiparallel to each other according to the sign of the intra-chain exchange interaction. The spins of different chains are kept parallel to each other, according to the bulk ferromagnetism of the compounds.

With this procedure the dipolar energies for the four Mn(hfac)₂(NITR) compounds are calculated as shown in Table 1. The z direction is the chain direction. y is chosen to lie in the Mn-R plane for cis coordinated complexes. In agreement with the considerations above both Mn(hfac)₂(NITPhOMe) and Mn(hfac)₂(NITiPr) have XY anisotropy, while Mn(hfac)₂(NITEt) has Ising anisotropy. Mn(hfac)₂(NITiPr) has a smaller dipolar energy compared to the former anisotropy. Mn(hfac)₂(NITiPr), essentially because the trigonal symmetry of the spins. Since the J values for the two compounds are rather similar, the calculated critical temperatures follow the same pattern as the dipolar energies, and as the experimental temperatures. The calculated critical temperature of Mn(hfac)₂(NITEt) falls in between the other two, while experimentally it has the highest Tc. However the Ising anisotropy actually must yield a higher spin correlation length then XY anisotropy, therefore increasing the critical temperature.

The satisfactory explanation of the short range order effects and of the critical temperatures using a simple dipolar approach, shows which is the main problem in this class of materials, if high Tc's must be arrived at. Further although in the cases reported in this Section the dipolar determined three dimensional order is ferromagnetic, this is by no means the rule and antiferromagnetic spin arrangements can arise depending on the preferred spin

orientation in the chains and on the relative disposition of the chains. This will be shown in the next section.

4.2 Copper Chains
Two structurally characterized copper(II)-nitronyl nitroxide chains were reported, Cu(hfac)₂(NITiPr) and Cu(hfac)₂(NITMe) [26,27]. Although the coordination of copper(II) is similar in both compounds, the ways in which the chains assemble in the cells are completely different, as shown in Figure 11. In Cu(hfac)₂(NITMe) all the chains are parallel to each other, while they are orthogonal to each other in Cu(hfac)₂(NITiPr).

Both compounds behave as one-dimensional ferromagnets and the susceptibility down to ca. 3 K could be satisfactorily reproduced using the formulae appropriate [39] to one-dimensional ferromagnets.
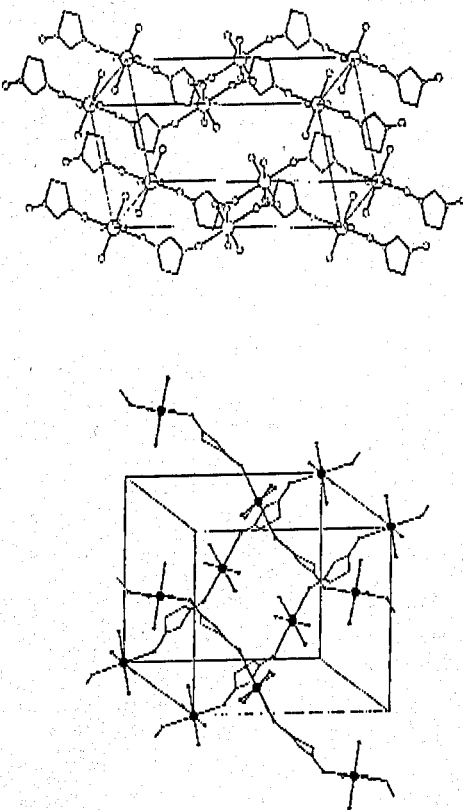
Figure 11. Crystal lattices of Cu(hfac)₂(NITMe), left, and Cu(hfac)₂(NITiPr), right.

At lower temperature some small deviations from one-dimensional behavior was observed, which could be satisfactorily fitted down to 1.2 K using the equation [40]:

$$\chi = \frac{\chi_{chn}}{1 + (zJ'/C)\chi_{chn}} \quad (7)$$

where $C = N\mu_B g^2$, χ_{chn} is the susceptibility appropriate to isolated chains, J' is

DA: BIBLIOTECA DI FISICA UNIMI   N. FAX :02 50317752   10 LUG. 2012 10:09   P 7

the inter-chain exchange interaction, and z is the number of nearest neighbor chains. The best fit parameters are $J = -24.5$ cm^{-1}, $zJ' = -2\times10^{-3}$ for Cu(hfac)$_2$(NITPr), and $J = -30.8$ cm^{-1}, $zJ' = 4.6\times10^{-2}$ cm^{-1} for Cu(hfac)$_2$(NITMe). The data for the latter show that an antiferromagnetic interaction is taking over at low temperature, while the small value observed for the former does not allow us to draw any safe conclusion.

Although in (7) we formally treat the inter-chain interaction as exchange in nature, qualitatively the same behavior of the average susceptibility might be arrived at also using a dipolar interaction. As a matter of fact, using the latter approach it is possible to rationalize the different behavior of ferrimagnetic manganese chains, which show order ferromagnetically, and of ferromagnetic chains which show antiferromagnetic deviations from ideal one-dimensional behavior.

As previously stated the preferred spin orientation for ferrimagnetic chains is orthogonal to the chain, while it is parallel to the chain for ferromagnetic chains. The dipolar field generated by a generic spin on one chain in the one-dimensional ferrimagnets tends to keep the corresponding spins on a neighboring chain parallel to itself as shown in Figure 12b. On the other hand, the dipolar field generated by a spin on a ferromagnetic chain tends to keep the spins on a neighboring chain antiparallel to itself, as shown in Figure 12a. Of course this behavior depends also on the offset of the neighboring chains relative to each other.
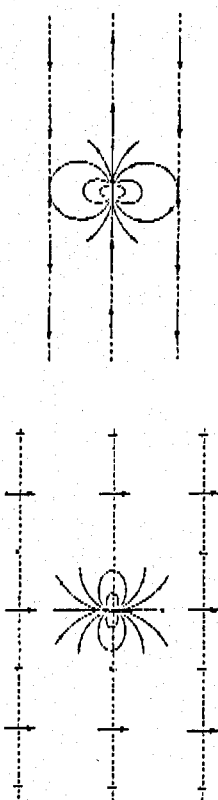
Figure 12. Dipolar fields generated by ferromagnetic and ferrimagnetic chains.

5. Beyond One-Dimensional Magnets

There is no doubt that the strong magnetic interactions between metal ions and nitronyl nitroxides make these two building blocks extremely appealing. However no substantial increase in Tc can be expected if the strong interactions are not extended to at least two dimensions. In order to achieve this goal we are currently using two approaches.

The first approach is that of introducing in the NITR radical additional donor atoms, which can in principle branch different chains. The radical which we have tested up to now is NITpPy [41,42], which we found to be able to coordinate both as bidentate, with the pyridine nitrogen and one NO group as donors, or as tridentate. What is interesting is that when the pyridine nitrogen binds to a

metal a moderate magnetic coupling is observed between the metal ion and the radical. J has been found to be 19.4 cm^{-1} for copper(II) [41], 10 cm^{-1} for nickel(II), and -1 cm^{-1} for manganese(II) [42].

When NITpPy acts as indentate ligand it can form chains as shown in Figure 4d. We investigated [Cu(hfac)$_2$]$_3$[NITpPy]$_2$ [17] which behaves as a one-dimensional antiferromagnet. However it is possible to isolate compounds of formula [M(hfac)$_2$]$_2$M'(hfac)$_2$[NITpPy]$_2$, which would be examples of chains in which three different types of spins alternate regularly in space. Further we have not yet lost the hope that two-dimensional structures can be constructed in this way.

The second approach in order to increase the lattice dimensionality of metal-nitronyl nitroxide complexes is that of substituting the shielding hexafluoroacetylacetonate ligands with other ligands which can yield more connected structures. Some success was achieved with metal carboxylates, in which we have found structures based on the repeat unit shown in Figure 13 [16]. In this case the metal carboxylates provide the frame for a chain structure, and the nitronyl nitroxides have a free NO group which can connect different chains. We suspect that we achieved such a structure in [Mn(pfbz)$_2$]$_2$NITEt [43] where pfbz is pentafluorobenzoate. Unfortunately we were not able to grow suitable crystals for X-ray analysis. Both compounds undergo magnetic phase transition at ca. 25 K, showing hysteresis loops. The field dependence of the magnetization rules out a ferromagnetic phase transition, but leaves the possibility open for a weak ferromagnet. Indeed such a magnetic behavior might be compatible with an antiferromagnetic ordering of two-dimensional ferrimagnets.
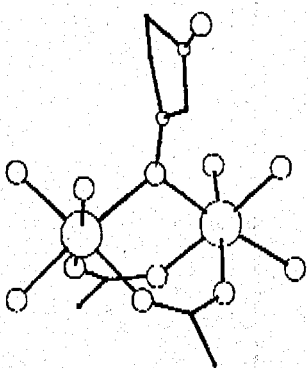
Figure 13. Repeat unit observed in metal carboxylate derivatives of nitronyl nitroxides.

6. Optical and Magnetic Properties

The characteristic of molecular magnetic materials which are in principle more desirable for possible applications are those related to magneto-optical properties. A well known magneto optical effect is the Faraday rotation, which is bound to the

fact that a magnetized specimen has a different refraction index for right and left circularly polarized light. Therefore a linearly polarized light beam propagating parallel to the direction of the magnetization rotates the polarization plane by an angle which depends on the nature of the material. For possible applications it would be desirable to have large specific rotation, and molecular materials in principle might be finely tuned through the usual chemical procedures to achieve this goal.

To our knowledge no data have been reported up to now on the Faraday rotation of molecular magnetic materials. However we want to notice that some of the molecular compounds reported to order ferromagnetically crystallize in the acentric space groups [44,37], therefore they should be optically active also in the paramagnetic state. It would be very interesting to investigate the interplay of the two types of optical activity (magnetic and natural) in these compounds, which offer a unique testing ground for theoretical models. Further, non-centric materials may be suitable for non-linear optical applications, like second harmonic generation. In fact we observed sizeable second harmonic generation in Mn(hfac)$_2$(NITPhOMe) [37], although we cannot provide a definitive value to χ^2 due to the fact that our compound absorbs the generated second harmonic when irradiated at 1064 nm. Again the interplay of optical and magnetic properties is a new field of research which deserves accurate investigations.

Another possible application of molecular magnetic materials might be associated with the presence of exciton—magnon side bands in the ordered phase, similar to these which are currently studied for application in magnetic garnets [45].

Our experience has been limited up to now to studies on simple metal—radical complexes, of which Cr(CTH)(DTBSQ){ CTH = rac-5,7,7,12,14,14-hexamethyl-1,4,8,11-tetraazacyclotetradecane; DTBSQ = 3,5-di-tert-butyl-semiquinone) is an illuminating example [46]. This compound has a ground S = 1 state, which originates from the strong antiferromagnetic interaction between chromium(III) and the semiquinone (J > 400 cm⁻¹). The chromium spin forbidden band $^4T_{1g} \rightarrow {}^2E_g$, which occurs at ca. 14,000 cm⁻¹ in most chromium complexes with very low intensity is observed in Cr(CTH)(DTBSQ) with ϵ = 3000 (cm⁻²mmol) due to the strong exchange coupling between the metal and the radical. Definitely more experimental work is needed in this area.

7. References

1) J.S. Miller; A.J. Epstein; W.M. Reiff, *Acc. Chem. Res.*, 1988, *21*, 114.
2) J.S. Miller; A.J. Epstein; W.M. Reiff, *Chem. Rev.*, 1988, *88*, 201.
3) Kahn, O. in "*Organic and Inorganic Low Dimensional Crystalline Materials*". Delhaes, P.; Drillon, M. Eds; NATO ASI Series B, 168, Plenum Press, New York, 1987, P. 93.
4) Torance, J.B.; Bagus, P.S.; Johannsen, I.; Nazzal, A.I.; Parkin, S.S.P.; Batail, P.; *J. Appl. Phys.*, 1988, *63*, 2962.
5) Ovchinnikov, A.A. *Theor. Chim. Acta*, 1978, *47*, 297.
6) *Mol. Cryst. Liq. Cryst*, 1989, *176*.
7) Iwamura, H. *Pure Appl. Chem.*, 1986, *58*, 187.
8) Caneschi, A.; Gatteschi, D.; Sessoli, R. *Acc. Chem. Res*, 1989, *22*, 392.
9) Mattis, D.C. "*The Theory of Magnetism*", Springer—Verlag, Berlin, 1981.
10) Renard, J.P. in "*Organic and Inorganic Low Dimensional Crystalline*

Materials" Delhaes, P.; Drillon, M. Eds.; NATO ASI Series B, 168, Plenum Press, New York, 1987, P. 125.
11) Morrish, A.H. "*The Physical Principles of Magnetism*", Wiley, New York, 1966.
12) Kanamori, J. in "*Magnetism*", Rado, T.G.; Suhl, H., Eds.; Academic Press, New York, vol. 1, 1963 p. 161.
13) Bencini, A.; Gatteschi, D. "*EPR of Exchange Coupled Systems*", Springer Verlag, Berlin, 1990.
14) Villain, J.; Loveluck, J.M. *J. Phys. Lett*, 1977, *38*, 177.
15) Caneschi, A.; Gatteschi, D.; Rey, P.; *Progr. Inorg. Chem.*, in press.
16) Caneschi, A.; Gatteschi, D.; Melandri, M.C.; Rey, P.; Sessoli, R. *Inorg. Chem.*, 1990, *29*, 4228.
17) Caneschi, A.; Ferraro, F.; Gatteschi, D.; Rey, P.; Sessoli, R. *Inorg. Chem.*, in press.
18) Caneschi, A.; Gatteschi, D.; Sessoli, R.; Cabello, C.I.; Rey, P.; Barra, A.L.; Brunel, L.C. *Inorg. Chem.*, in press.
19) Benelli, C.; Caneschi, A.; Gatteschi, D.;Pardi, L.; Rey, P. *Inorg. Chem.*, 1989, *28*, 3230.
20) Hatfield, W.E.; Estes, W.E.; Marsh, W.E.; Pickens, M.W.; ter Haar, L.W.; Weller, R.R. in "*Extended Linear Chain Compounds*", Miller, J.S. Ed.; Plenum Press, New York, vol. 3, 1983, p. 43.
21) Cogne, A.; Grand, A.; Rey, P.; Subra, R. *J. Am. Chem. Soc.*, 1989, *111*, 3230.
22) Richards, P.M. in "*Local Properties at Phase Transitions*", Muller, K.A.; Rigamonti, A., Eds.; Editrice Composition; Bologna, 1975.
23) Gatteschi, D.; Sessoli, R. *J. Magn. Res. Rev.*, 1990, *15*, 1.
24) Nagata, K.; Tazuke, Y. *J. Phys. Soc. Japn.*, 1972, *32*, 377.
25) Karasudani, T.; Okamoto, H. *J. Phys. Soc. Japn.*, 1977, *43*, 1131.
26) Caneschi, A.; Gatteschi, D.; Laugier, J.; Rey, P. *J. Am. Chem. Soc.*, 1987, *109*, 2191.
27) Cabello, C. I.; Caneschi, A.; Carlin, R.L.; Gatteschi, D.; Rey, P.; Sessoli, R. *Inorg. Chem.*, 1990, *29*, 2582.
28) Caneschi, A.; Gatteschi, D.; Zanchini, C.; Rey, P. *J. Chem. Soc. Faraday Trans.*, 1987, *83*, 3603.
29) Caneschi, A.; Gatteschi, D.; Rey, P.; Sessoli, R. *Inorg. Chem.*, 1988, *27*, 1756.
30) Caneschi, A.; Gatteschi, D.; Renard, J.P.; Rey, P.; Sessoli, R. *Inorg. Chem.*, 1989, *28*, 1976.
31) Caneschi, A.; Gatteschi, D.; Renard, J.P.; Rey, P.; Sessoli, R. *Inorg. Chem.*, 1989, *28*, 3314.
32) Caneschi, A.; Gatteschi, D.; Renard, J.P.; Rey, P.; Sessoli, R. *Inorg. Chem.*, 1989, *28*, 2940.
33) Georges, R.; Curely, J.; Drillon, M. *J. Appl. Phys.*, 1985, *58*, 914.
34) Drillon, M.; Coronado, E.; Beltran, D.; Georges, R. *Chem. Phys.*, 1983, *79*, 449.
35) Seiden J. *J. Phys. Lett*, 1983, *44*, 1947.
36) Verdaguer, M.; Julve, M.; Michalowicz, A.; Kahn, O. *Inorg. Chem.*, 1983, *22*, 2624.
37) Caneschi, A.; Gatteschi, D. Rey, P.; Sessoli, R. submitted for publication.
38) Manuscript in preparation.
39) Baker, G.H. Jr.; Rushbrooke, G.S.; Gilbert, H.E. *Phys. Rev*, 1964, *A135*, 1272.

40) Hatfield, W.E.; Weller, R.R.; Hall, J.W. *Inorg. Chem.*, 1980, 19, 3825.

41) Caneschi, A.; Ferraro, F.; Gatteschi, D.; Rey, P.; Sessoli, R. *Inorg. Chem.*, 1990, 29, 1756.

42) Caneschi, A.; Ferraro, F.; Gatteschi, D.; Rey, P.; Sessoli, R. *Inorg. Chem.*, 1990, 29, 4217.

43) Caneschi, A.; Gatteschi, D.; Renard, J.P.; Rey, P.; Sessoli, R. *J. Am. Chem. Soc.*, 1989, 111, 785.

44) Pei, Y.; Verdaguer, M.; Kahn, O.; Sletten, J.; Renard, J. P. *J. Am. Chem. Soc.*, 1986, 108, 7428.

45) Tsushima, K. in "*Physics of Magnetic Materials*", Rautuszkiiewicz, J.; Szymczak, H.; Lachowicz, H.K., Eds.; World Scientific, Singapore, Philadelphia, 1985, p. 479.

46) Benelli, C.; Dei, A.; Gatteschi, D.; Gudel, H. U.; Pardi, L. *Inorg. Chem.*, 1989, 28, 3089.